


# Tuning the photoluminescence of MoS<sub>2</sub>/TiO<sub>2</sub> by molecular self-assembly films

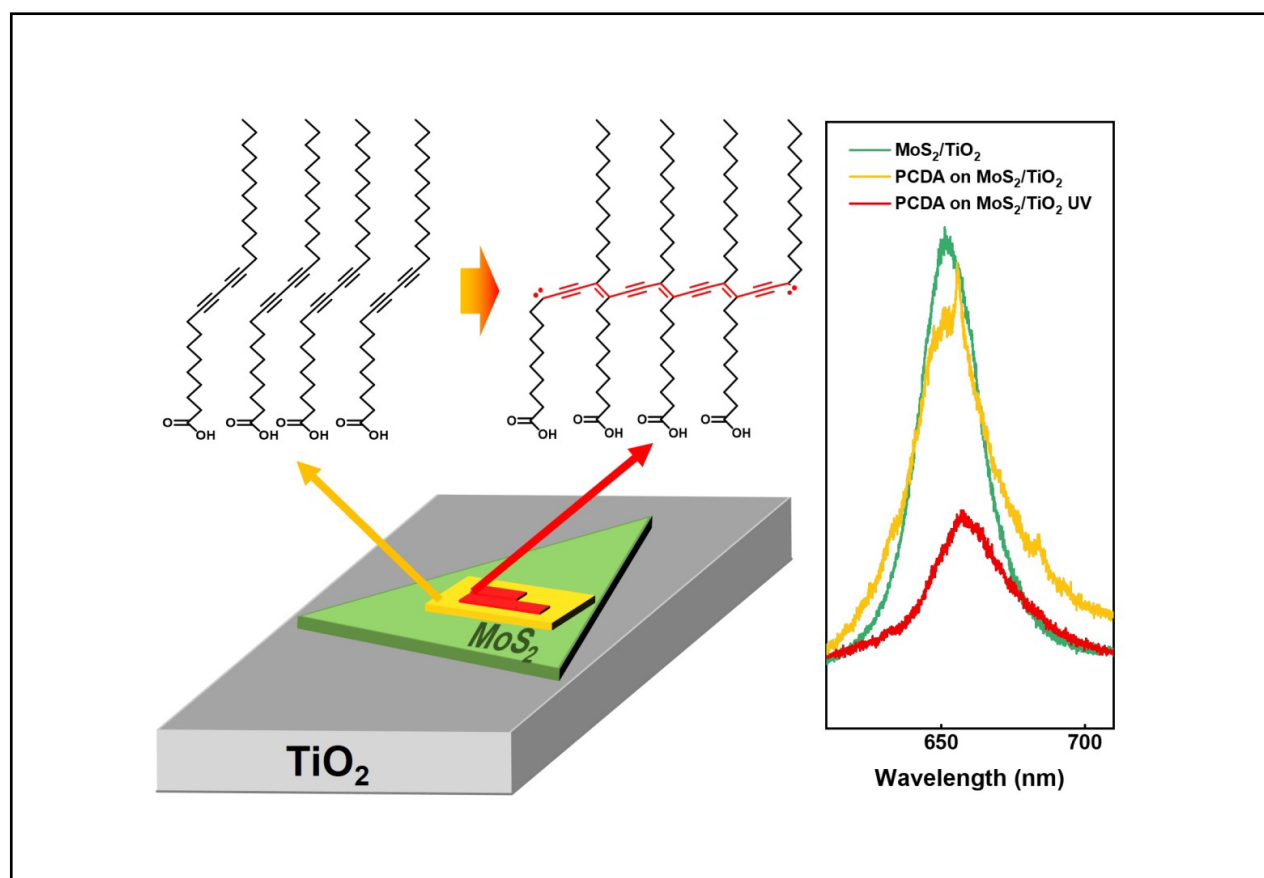
Hechenyu Zha, Yue Xing, Miaomiao Xiang, and Xiang Shao 

Department of Chemical Physics, University of Science and Technology of China, Hefei 230026, China

 Correspondence: Xiang Shao, E-mail: [shaox@ustc.edu.cn](mailto:shaox@ustc.edu.cn)

© 2023 The Author(s). This is an open access article under the CC BY-NC-ND 4.0 license (<http://creativecommons.org/licenses/by-nc-nd/4.0/>).

## Graphical abstract



*Self-assembly films of PCDA and its in situ photopolymerization donate different amount of electrons to the MoS<sub>2</sub>/TiO<sub>2</sub> surface and thus modulate the photoluminescence of the latter.*

## Public summary

- Monolayer MoS<sub>2</sub> was grown on rutile TiO<sub>2</sub>(110) single crystal through an ambient CVD method.
- PCDA assembles into lamellae structure on the MoS<sub>2</sub>/TiO<sub>2</sub> surface and polymerizes in situ under the UV irradiation.
- The assembled and the further polymerized PCDA molecules donate electrons to the MoS<sub>2</sub>/TiO<sub>2</sub> and tune the photoluminescence of the latter.

# Tuning the photoluminescence of MoS<sub>2</sub>/TiO<sub>2</sub> by molecular self-assembly films

Hechenyu Zha, Yue Xing, Miaomiao Xiang, and Xiang Shao 

Department of Chemical Physics, University of Science and Technology of China, Hefei 230026, China

✉ Correspondence: Xiang Shao, E-mail: [shaox@ustc.edu.cn](mailto:shaox@ustc.edu.cn)

© 2023 The Author(s). This is an open access article under the CC BY-NC-ND 4.0 license (<http://creativecommons.org/licenses/by-nc-nd/4.0/>).

Cite This: *JUSTC*, 2023, 53(12): 1206 (8pp)


Read Online

**Abstract:** Self-assembly films have demonstrated an efficient method to functionalize the surfaces of variously different materials. In this work, we preliminarily explored the modification effect of 10,12-pentacosadiynoic acid (PCDA) on the optical properties of monolayer molybdenum disulfide (MoS<sub>2</sub>) grown on a rutile titanium dioxide (r-TiO<sub>2</sub>) (110) single crystal surface. Atomic force microscopy (AFM) characterizations directly revealed that the PCDA molecules self-assemble into the same lamella structure as on pure MoS<sub>2</sub>, which can be further polymerized into conductive polydiacetylene (PDA) chains under ultraviolet light (UV) irradiation. Detailed photoluminescence (PL) measurements observed clearly increased luminescence of negative trions (A<sup>-</sup>) yet decreased total intensities for MoS<sub>2</sub> upon adding the PCDA assembly, which is further enhanced after stimulating its polymerization. These results indicate that the PCDA assembly and its polymerization have different electron donability to MoS<sub>2</sub>, which hence provides a deepened understanding of the interfacial interactions within a multicomponent system. Our work also demonstrates the self-assembly of films as a versatile strategy to tune the electronic/optical properties of hybridized two-dimensional materials.

**Keywords:** 10,12-pentacosadiynoic acid; MoS<sub>2</sub>/TiO<sub>2</sub>; self-assembly; photopolymerization; photoluminescence

CLC number: O644.1

Document code: A

## 1 Introduction

Recently, transition metal dichalcogenides (TMDs) have attracted immense research attention owing to their superior properties, including their layered structure, outstanding electrical conductivity and optical properties, and have been implemented in a wide range of applications, such as electronics, optics, sensors and heterogeneous catalysis<sup>[1–3]</sup>. In particular, when integrated with active oxide semiconductors, such as TiO<sub>2</sub>, the combinative system has been discovered with enhanced electro or photocatalytic performances<sup>[4–6]</sup> and thus has drawn intensive attention due to its expandable potential in electronics, photovoltaics, and photocatalysis. In the past several years, our group has developed an ambient-pressure chemical vapor deposition (CVD) method to grow high-quality single-layer MoS<sub>2</sub> on differently terminated rutile TiO<sub>2</sub> single crystals to successfully construct model hybridized MoS<sub>2</sub>/TiO<sub>2</sub> systems with ideally controlled interfaces<sup>[7,8]</sup>. Based on the series of characterizations, we revealed that the subtle change in the atomic structure of the interface may significantly influence the optical properties of the combination system. Moreover, under most application conditions, the MoS<sub>2</sub>/TiO<sub>2</sub> structure will be further integrated with other functional materials. In this case, the interactions between multiple interfaces must be carefully considered.

Organic self-assembly films (SAMs) have been demonstrated as an effective method to modify various surfaces in recent decades<sup>[9,10]</sup>. In fact, SAMs are also frequently applied

in solar cells or photovoltaic devices<sup>[11,12]</sup>. Nevertheless, the detailed interactions between SAMs and the surfaces of functional semiconductors are not yet well understood, particularly for heterostructures comprising ultrathin two-dimensional materials (2DM). In this work, we investigated for the first time the assembly behavior of a prototypical photosensitive molecule, 10,12-pentacosadiynoic acid (PCDA, see Fig. 1), on the surface of the MoS<sub>2</sub>/TiO<sub>2</sub> heterostructure. PCDA has been demonstrated to assemble into lamella structures on various surfaces<sup>[13,14]</sup>. The aligned diacetylene groups can be further polymerized into linear conductive chains under ultraviolet (UV) light irradiation or pulse excitation and thus are considered promising candidates for molecular conductors<sup>[15]</sup>. Our atomic force microscopy (AFM) characterizations demonstrate that the PCDA molecules form the same assembly structure on the MoS<sub>2</sub>/TiO<sub>2</sub> surface as on the pure MoS<sub>2</sub> substrate and can also be triggered to polymerize upon UV irradiation. However, the molecular film and its reaction product have different effects on the photoluminescence of MoS<sub>2</sub>, which can be attributed to the different charge transfer conditions at the interface. These results may shed new light on the interface interactions between functional organic SAMs and hybridized semiconductive materials.

## 2 Materials and methods

### 2.1 Preparation of the MoS<sub>2</sub>/TiO<sub>2</sub> substrate

The monolayer MoS<sub>2</sub>/TiO<sub>2</sub> substrate was prepared with the



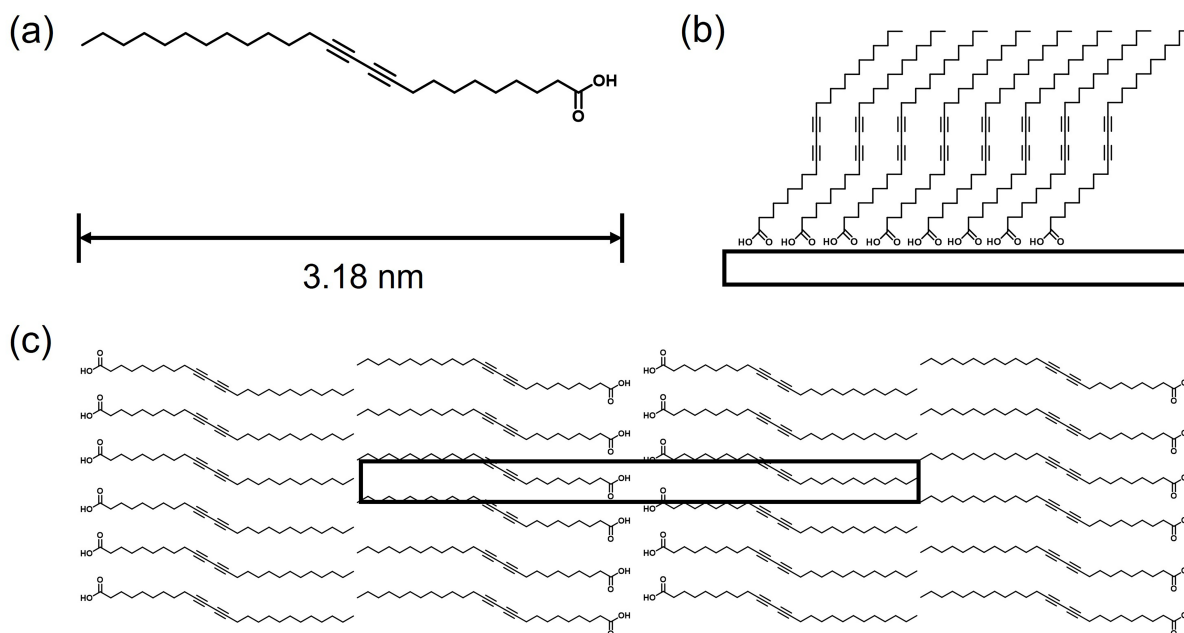


**Fig. 1.** (a) Molecular structure of 10,12-pentacosadiynoic acid. (b, c) The standing-up and flat-lying assembly structures of PCDA on oxide and other inert substrates, respectively. The rectangle in (c) marks the unit cell.

same recipe reported previously by our group<sup>[7,8]</sup>. As the first step, the received rutile TiO<sub>2</sub>(110) single crystal (Hefei Kejing Materials Technology Co., Ltd.) was etched with HF solution, followed by annealing in air to obtain an atomically flat surface. Then, the as-prepared TiO<sub>2</sub> substrate was loaded into the high-temperature zone of a two-zone tube furnace (Hefei Kejing Materials Technology Co., Ltd.). After that, 120 mg of sulfur powder (Shanghai Aladdin Biochemical Technology Co., Ltd., 99.95%) was weighed in a quartz boat and placed in the upstream low-temperature zone of the tube furnace, where the temperature was set at 200 °C. Meanwhile, 6 mg of molybdenum trioxide (MoO<sub>3</sub>, Shanghai Aladdin Biochemical Technology Co., Ltd., 99.95%) was weighed in another quartz boat and placed approximately 2 cm downstream against the TiO<sub>2</sub> substrate. When everything was assembled, pure nitrogen gas was introduced at a gas rate of 300 sccm for 30 min to flush out the residual air and to ensure an inert gas environment during the reaction process. After that, the nitrogen flow rate was lowered to 100 sccm, and the high-temperature zone was gradually heated to ~750 °C at a speed of 15 °C/min to ensure that both the S and MoO<sub>3</sub> precursors reached their sublimation temperature at roughly the same time. For the samples used in this study, the reaction was maintained for ~10 min. As a result, we could fabricate uniformly distributed monolayer MoS<sub>2</sub> flakes as large as 1 μm for the side width while perfectly maintaining the atomic flatness of the surface, as will be presented below.

## 2.2 Preparation of the PCDA assembly films

All chemicals were used as received without further purification. The PCDA molecule (Shanghai Aladdin Biochemical Technology Co., Ltd., 97%) was dissolved in toluene (Sino-pharm Chemical Reagent Co., Ltd., analytical purity) until the concentration reached  $1.0 \times 10^{-5}$ – $1.0 \times 10^{-4}$  mol/L. The PCDA/toluene solutions were carefully stored in brown

volumetric flasks and renewed after a few days. To prepare the SAMs on different substrates, 10 μL of solution was drop cast onto the MoS<sub>2</sub> or MoS<sub>2</sub>/TiO<sub>2</sub> surface and kept under the cover of a beaker for a few minutes until the solvent completely evaporated. Commercial single-crystal MoS<sub>2</sub> (Hefei Kejing Materials Technology Co., Ltd.,  $15 \times 15 \times 1$  mm<sup>3</sup>) was cut into small squares (~5 mm × 5 mm width) before use. To prepare a clean surface, the top layers of the MoS<sub>2</sub> crystal were either peeled off with tape or mechanically cleaved with a clean knife. In contrast, the MoS<sub>2</sub>/TiO<sub>2</sub> substrate was directly used without further cleaning. All samples were characterized immediately after preparation. For the UV irradiation experiments, a UV lamp (TANK007, UV-AA01) with a wavelength centered at 365 nm and a power of 3 W was used, which was kept ~3 cm from the sample surface and illuminated for 5–10 min to stimulate the polymerization of PCDA. No obvious temperature rise of the sample was found.

## 2.3 Characterization methods

All microscopic measurements were acquired on a Digital Instruments NanoScope IIIa MultiMode™ system under ambient conditions. AFM images were acquired using a silicon cantilever probe (VTESPA-300, Bruker). Scanning tunneling microscopy (STM) images were acquired using a Pt/Ir tip prepared by mechanical cutting from a 0.25 mm platinum-iridium wire (Alfa Aesar). The STM experiments were only successfully performed for PCDA on the pure MoS<sub>2</sub> surface, wherein a commercial MoS<sub>2</sub> crystal (Hefei Kejing Materials Technology Co., Ltd.) was used as the substrate. Unfortunately, STM measurements of PCDA on MoS<sub>2</sub>/TiO<sub>2</sub> did not succeed owing to the lack of sufficient conductivity. Photoluminescence (PL) measurements were carried out using a laser Raman spectrometer system from LabRamHR Evolution (JY, France). The incident laser beam has a wavelength of 532 nm and a power of 1.5 mW. The diameter of the focus is

approximately 1  $\mu\text{m}$ , which ideally fits the size of our as-grown  $\text{MoS}_2$ . The integration time is normally set as 10 s.

### 3 Results and discussion

#### 3.1 Characterization of the as-prepared $\text{MoS}_2/\text{TiO}_2$ substrate

As stated in the experimental section, the  $\text{MoS}_2/\text{TiO}_2$  substrate was fabricated through the ambient-pressure CVD recipe developed in our own group<sup>[8,16]</sup>. In Fig. 2, we present the main characterization results of the  $\text{MoS}_2/\text{TiO}_2$  sample. Fig. 2a displays the AFM image of the bare  $\text{TiO}_2$  surface before CVD synthesis of  $\text{MoS}_2$ , which shows atomically flat terraces as wide as  $\sim 200$  nm and separated by monoatomic steps ( $\sim 0.34$  nm for the height)<sup>[17]</sup>. After the CVD synthesis, the AFM image in Fig. 2b clearly shows a triangular-shaped monolayer  $\text{MoS}_2$  flake overlapping on the  $\text{TiO}_2$  surface while perfectly maintaining the surface flatness and cleanliness. The inserted section profile across the  $\text{MoS}_2$  boundary directly reads the height of the  $\text{MoS}_2$  flake as  $\sim 0.71$  nm, demonstrating its monolayer thickness<sup>[8]</sup>. Meanwhile, the step features of  $\text{TiO}_2$  underneath  $\text{MoS}_2$  can also be clearly observed, indicating that both materials have intimate contact. Fig. 2c shows a typical SEM image of the as-grown sample, manifesting the uniformly high quality of the fabricated  $\text{MoS}_2$ , each having an average size of  $\sim 1 \mu\text{m}$ .

In addition to this microscopic evidence, we also performed spectroscopy measurements to characterize the  $\text{MoS}_2/\text{TiO}_2$  sample. The Raman spectrum was taken on the special sample prepared by transferring the as-grown  $\text{MoS}_2$  onto a  $\text{SiO}_2/\text{Si}$  substrate. This is done because  $\text{TiO}_2$  has very

strong Raman features overlapping with and hence covering those for the  $\text{MoS}_2$  adlayer. The spectrum in Fig. 2d clearly shows the typical  $E_{2g}^1$  and  $A_{1g}$  features of  $\text{MoS}_2$  positioning at  $385.99 \text{ cm}^{-1}$  and  $405.58 \text{ cm}^{-1}$ , respectively. The wavenumber difference between the two peaks was found to be  $19.59 \text{ cm}^{-1}$  ( $< 20 \text{ cm}^{-1}$ ), which also provides additional evidence for the monolayer thickness of the as-grown  $\text{MoS}_2$ <sup>[18,19]</sup>. Fig. 2e and 2f show the XPS spectra of the  $\text{MoS}_2/\text{TiO}_2$  sample. The Mo high-resolution XPS spectrum clearly displays two distinct peaks positioned at  $231.65 \text{ eV}$  and  $234.55 \text{ eV}$ , which are consistent with the  $\text{Mo}^{4+} 3d_{5/2}$  and  $\text{Mo}^{4+} 3d_{3/2}$  components of  $\text{MoS}_2$ , respectively, as reported in the literature<sup>[20,21]</sup>. Correspondingly, the S 2p spectrum in Fig. 2f also confirms the existing oxidation state of sulfur as  $-2$ <sup>[22]</sup>. Quantitative elemental analysis reveals that the S/Mo ratio is approximately 2.1, indicating that a nearly stoichiometric  $\text{MoS}_2$  crystal has been fabricated on  $\text{TiO}_2$ .

#### 3.2 Self-assembly of PCDA on the $\text{MoS}_2$ surface

The self-assembly of PCDA and similar derivatives on the  $\text{MoS}_2$  surface has been extensively investigated previously<sup>[14,23]</sup>. Fig. 3 presents our own experimental data of PCDA on  $\text{MoS}_2$ , providing a reference for the study of PDCA on  $\text{MoS}_2/\text{TiO}_2$ . As shown in Fig. 1c, on inert surfaces such as graphite and  $\text{MoS}_2$ , the PCDA molecules tend to lie down and assemble into a lamellar structure wherein the diacetylene groups are aligned into chains. Here, our AFM scanning (Fig. 3a) also clearly recognizes the chain-like structures, which are representative of the PCDA molecular rows with an interval of approximately 7 nm. The ambient STM characterization in Fig. 3b directly resolves each PCDA molecule in the rows.

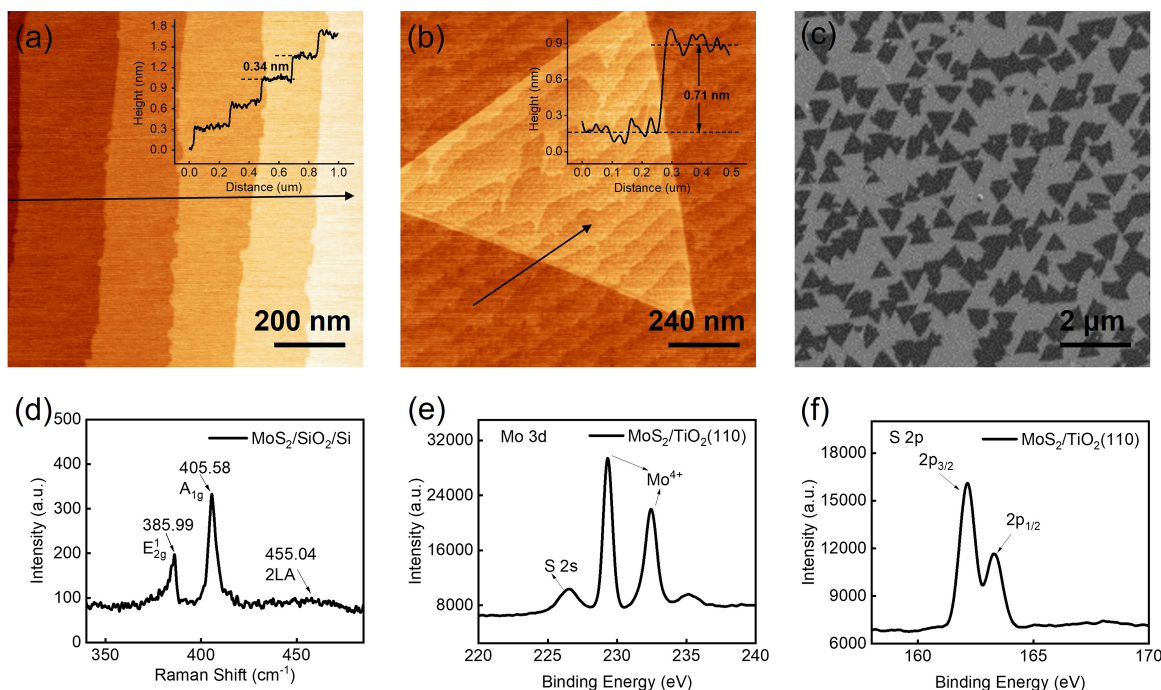


**Fig. 2.** Characterization of the as-prepared  $\text{MoS}_2/\text{TiO}_2$  substrate. (a) AFM image of an atomically flat  $\text{TiO}_2(110)$  surface. The inset in the upper right corner shows the profile taken along the black arrow. (b) AFM image of a triangular  $\text{MoS}_2$  flake on the  $\text{MoS}_2/\text{TiO}_2$  surface. The upper right inset shows the height profile measured across the  $\text{MoS}_2$  boundary along the black arrow. (c) Typical SEM image of the as-prepared  $\text{MoS}_2/\text{TiO}_2$  surface. (d) Raman spectrum of  $\text{MoS}_2$  transferred from  $\text{TiO}_2$  onto a  $\text{SiO}_2/\text{Si}$  substrate. (e, f) High-resolution XPS spectra of Mo 3d and S 2p on  $\text{MoS}_2/\text{TiO}_2$ .

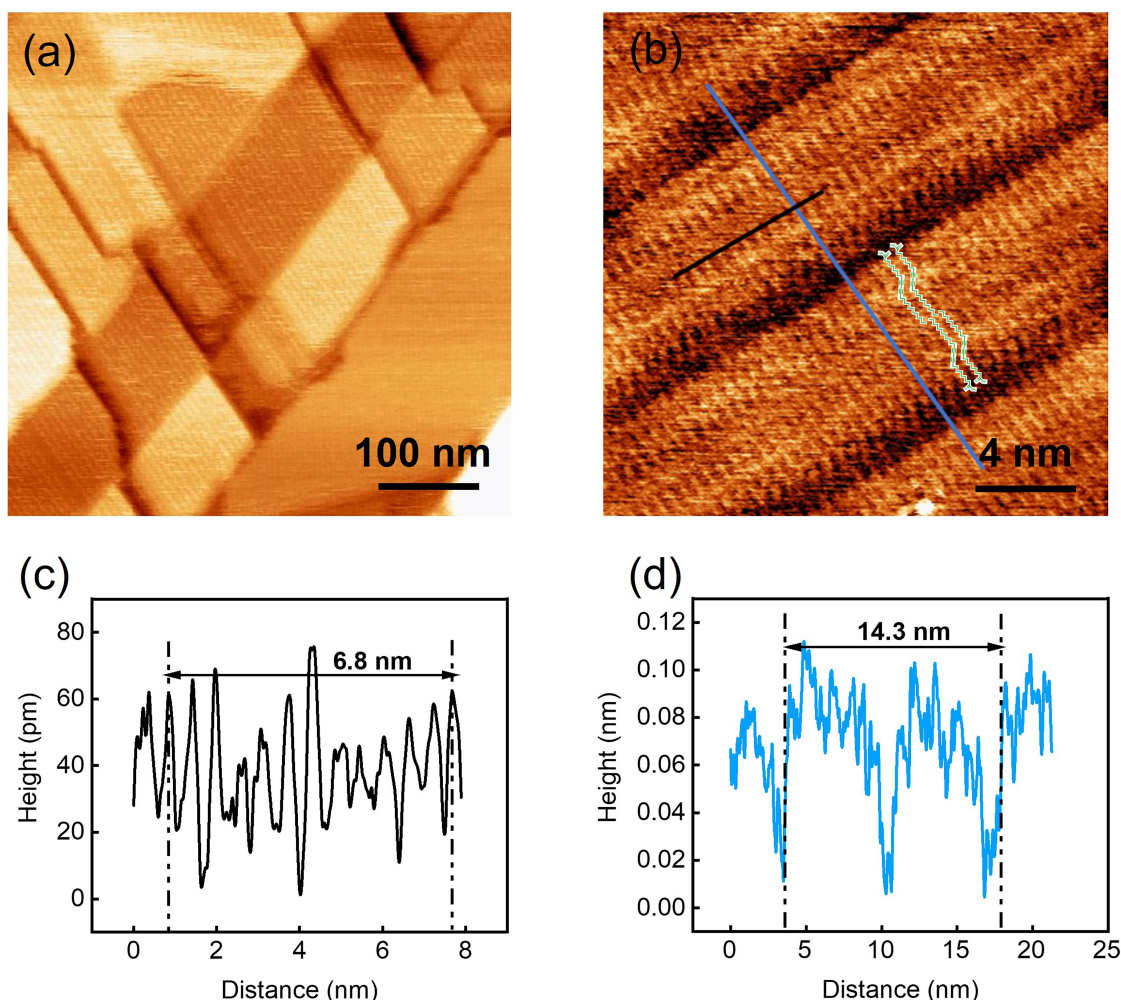


**Fig. 3.** (a) AFM and (b) the corresponding STM characterizations of the self-assembly film of PCDA formed on MoS<sub>2</sub>. Four PCDA molecular models are overlapped over the STM image. Note that although the film coverage slightly surpasses that of the monolayer, STM can only observe the structure of the bottom layer. (c, d) are the section profiles taken along the black and blue lines, respectively. The measured distances correspond to ten and double times the periodicities in these directions.

The bright regions correspond to the alkyl chains, including the diacetylene groups, while the dark troughs correspond to the hydrogen-bonded carboxylic end groups. Detailed profile analyses in Fig. 3c and 3d reveal that the width of the PCDA rows is  $\sim 7.1$  nm, in which the PCDA molecules are separated from each other with an interval of  $\sim 0.6$  nm. All these features are perfectly consistent with the literature report as well as the molecular models, as shown in Fig. 1<sup>[14]</sup>.

### 3.3 Self-assembly of PCDA on the MoS<sub>2</sub>/TiO<sub>2</sub> surface

After the PCDA test experiments on pure MoS<sub>2</sub>, we then tried to explore its assembly behavior on the MoS<sub>2</sub>/TiO<sub>2</sub> surface. Fig. 4a shows a typical AFM image of depositing 10  $\mu$ L of the PCDA/toluene ( $1 \times 10^{-4}$  mol/L) solution on a 5 mm $\times$ 10 mm MoS<sub>2</sub>/TiO<sub>2</sub> substrate. Interestingly, it was found that PCDA does not form a uniform film on the surface but instead forms distinct aggregates on the TiO<sub>2</sub> and MoS<sub>2</sub> regions. The rectangular-shaped tall islands correspond to the aggregates on the TiO<sub>2</sub> surface, which are proposed to be multiple layers of tilting PCDA molecules, as schemed in Fig. 1b. Although this is the first study to observe such PCDA assembly on the rutile TiO<sub>2</sub>(110) surface, we do not discuss it in detail but only

focus on the aggregates formed on the MoS<sub>2</sub> region. Fig. 4b shows the topographic AFM image covering a MoS<sub>2</sub> flake. It can be clearly seen that the deposited PCDA molecules have assembled into submonolayer films with a height of  $\sim 0.5$  nm. In addition, the zoomed-in phase image in Fig. 4c displays an obvious parallel-line pattern with a periodic interval of  $\sim 6.9$  nm (see the profile analysis in Fig. 4d). These characteristics demonstrate that the assembly structure of PCDA on the MoS<sub>2</sub>/TiO<sub>2</sub> surface should be exactly the same as that on the pure MoS<sub>2</sub> surface<sup>[24]</sup>. All the PCDA molecules lie on the surface and align their diacetylene groups together, as shown in the model in Fig. 1c. Such a flat-lying configuration of PCDA is not surprising considering that the MoS<sub>2</sub>/TiO<sub>2</sub> surface is also barely inert and cannot directly bond to the carboxylic end group of PCDA. However, such a configuration ensures direct contact of the diacetylene group with the MoS<sub>2</sub> surface and hence facilitates charge transfer between the two materials, as will be discussed later.

### 3.4 UV-stimulated polymerization of PCDA molecules on MoS<sub>2</sub>/TiO<sub>2</sub>

The most attractive property of the PCDA assembly is its



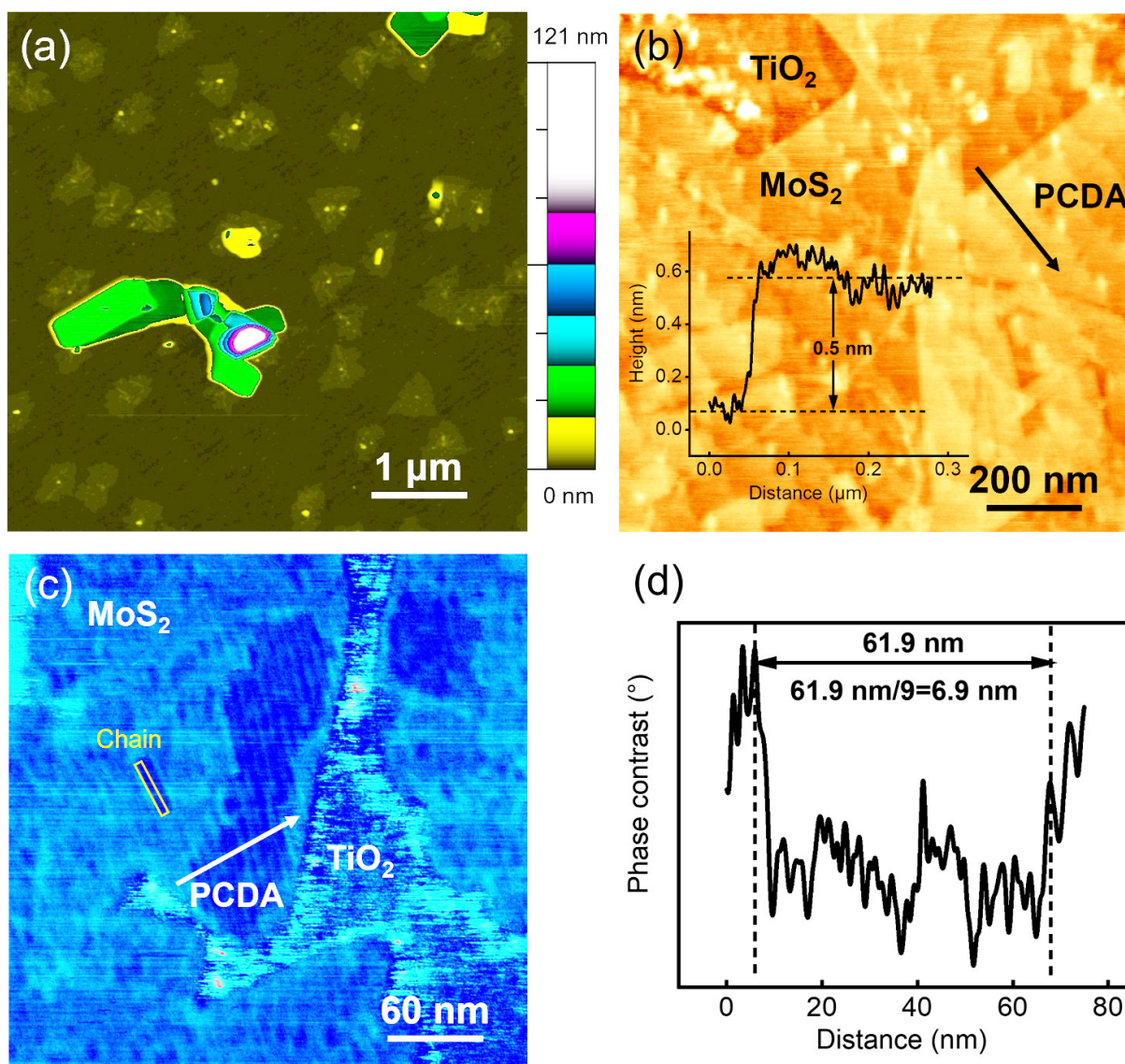


**Fig. 4.** AFM characterization of the assembly structure of PCDA on the MoS<sub>2</sub>/TiO<sub>2</sub> surface. (a) Large-area topographic image showing the PCDA aggregates formed on the MoS<sub>2</sub>/TiO<sub>2</sub> surface. (b) Zoomed-in topographic image focusing on the MoS<sub>2</sub>/TiO<sub>2</sub> region covered by PCDA film. (c) Zoomed-in phase image showing the resolved assembly structure of PCDA on MoS<sub>2</sub>/TiO<sub>2</sub>. (d) Section profile taken along the white arrow in (c), which measures the periodicity of the PCDA assembly as ~6.9 nm.

polymerization reaction under external excitations. Previous studies have demonstrated that PCDA on MoS<sub>2</sub> can be stimulated to polymerize upon UV irradiation<sup>[14]</sup>. However, whether this reaction can take place on MoS<sub>2</sub>/TiO<sub>2</sub> is still unknown. Therefore, we shed a 365 nm UV light onto the PCDA/MoS<sub>2</sub>/TiO<sub>2</sub> sample for ~10 min. As shown in Fig. 5a, it can be clearly seen that some brighter lines developed while part of the original lower ones are still observed. Their differences become more apparent when examining the corresponding phase image, as shown in Fig. 5b. These brighter chains are attributed to polymerized PCDA (PDA) on the MoS<sub>2</sub>/TiO<sub>2</sub> surface<sup>[15]</sup>. Their increased height (~0.14 nm, see Fig. 5c) relative to the unreacted PCDA molecules can be explained by the lifted poly-diacetylene groups, as shown by the inserted model in Fig. 5c. Aside from the polymerized PCDA films, we also noticed that the triangular MoS<sub>2</sub> flake and the TiO<sub>2</sub> surface remained unchanged, indicating that UV light

had a limited influence on these surface structures.

### 3.5 PL of the PCDA-covered MoS<sub>2</sub>/TiO<sub>2</sub> samples

The optical property is one of the most attractive properties of MoS<sub>2</sub><sup>[25,26]</sup>. To explore the effect of PCDA molecules on the photoluminescence of the MoS<sub>2</sub>/TiO<sub>2</sub> combinational system, we performed PL measurements on a series of PCDA/MoS<sub>2</sub>/TiO<sub>2</sub> samples. Fig. 6a–c presents mainly the A peaks of MoS<sub>2</sub> at approximately 650 nm, which is the most prominent PL signal resulting from the cross-band annihilation of the A excitons in MoS<sub>2</sub><sup>[16,27]</sup>. Based on the peak-fitting analysis, all the PL spectra can be divided into two components. The short wavelength component (in blue) is always dominant and can be attributed to the neutral A exciton, while the long wavelength component (in yellow) can be attributed to the negatively charged A exciton (A<sup>-</sup>)<sup>[28]</sup>. Detailed analysis found that both the intensity of PL and the intensity ratio of

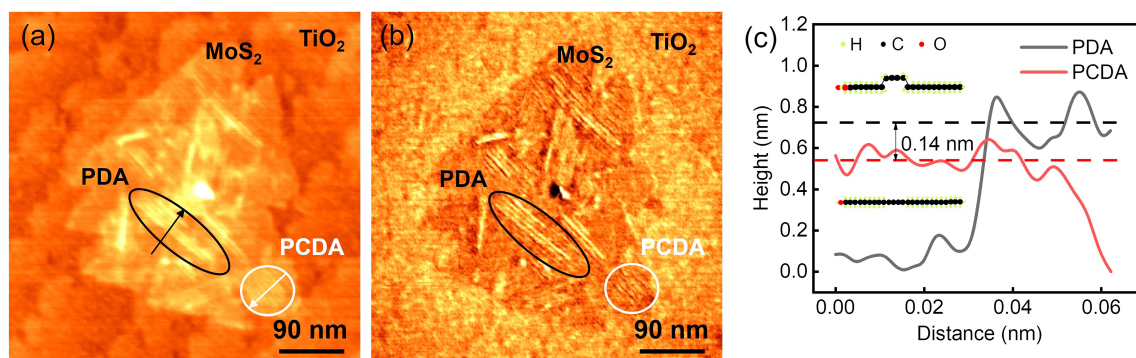


**Fig. 5.** (a) AFM topography and (b) the corresponding phase images of the PCDA/MoS<sub>2</sub>/TiO<sub>2</sub> surface after UV irradiation. The black and red ovals highlight the polymerized and unreacted PCDA assembly, respectively. (c) Section profiles taken along the black and red arrows in (a), showing the height difference between the reacted and unreacted PCDA film. Inserted are the simple schematics for the flat lying PCDA (lower) and the PDA polymer (upper), respectively.

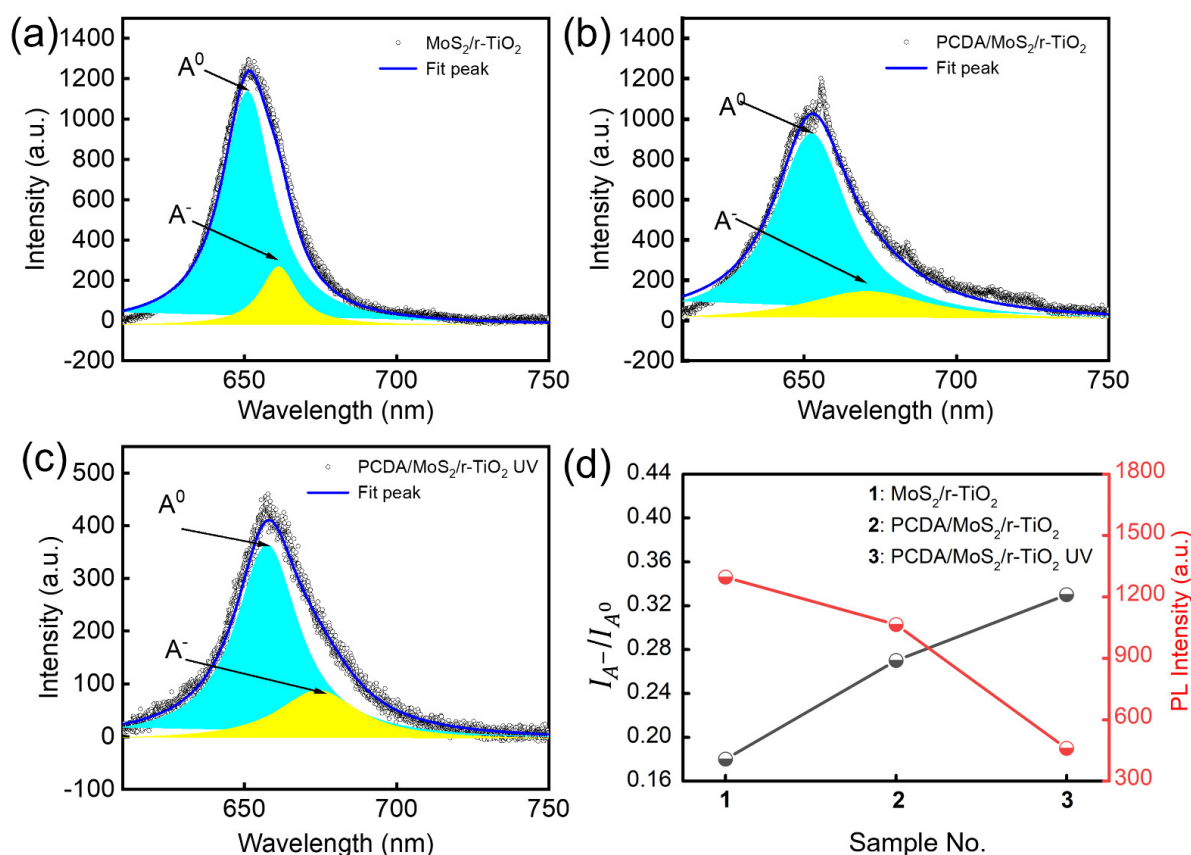


**Fig. 6.** PL spectra measured on the different samples: (a) bare MoS<sub>2</sub>/r-TiO<sub>2</sub>, (b) PCDA/MoS<sub>2</sub>/r-TiO<sub>2</sub> and (c) PCDA/MoS<sub>2</sub>/r-TiO<sub>2</sub> structure after UV irradiation. All the spectra are properly fit with two peaks, i.e., A<sup>0</sup> and A<sup>-</sup>. (d) Plot of the PL intensities and the  $I_{A^-}/I_{A^0}$  ratios versus different samples.

$A^-/A$  ( $I_{A^-}/I_{A^0}$ ) significantly vary for different samples. As summarized in Fig. 6d, the PL intensity is the largest for the bare MoS<sub>2</sub>/r-TiO<sub>2</sub> sample but consecutively decreases on PCDA/MoS<sub>2</sub>/r-TiO<sub>2</sub> and UV-illuminated PCDA/MoS<sub>2</sub>/r-TiO<sub>2</sub> (termed PCDA/MoS<sub>2</sub>/r-TiO<sub>2</sub>-UV). In contrast, the ratio of  $I_{A^-}/I_{A^0}$  reverses the ordering, indicating that the A<sup>-</sup> luminescence becomes increasingly prominent upon adding PCDA onto the MoS<sub>2</sub>/TiO<sub>2</sub> surface and stimulating its polymerization. Realizing that the A<sup>-</sup> exciton is a quasiparticle formed by

combining a neutral exciton with a free electron<sup>[28]</sup>, we propose that the number of free electrons in MoS<sub>2</sub> actually varies for these different PCDA/MoS<sub>2</sub>/TiO<sub>2</sub> samples. These free electrons may be donated from the PCDA assembly films. As revealed by the AFM measurements, the PCDA molecules take a flat-lying configuration on the MoS<sub>2</sub> surface, which means that their electron-donating diacetylene groups can directly contact the MoS<sub>2</sub> surface to efficiently transfer electrons into the latter. For polymerized PDCA, although the



poly-diacetylene groups are slightly lifted away from the surface, their conductive wire structure is much more beneficial for transporting electrons than the single molecules and thus may donate more electrons into MoS<sub>2</sub>. Along with the added electrons, the formation probability of the A<sup>-</sup> exciton in MoS<sub>2</sub> synchronically increases. Because the formation of each A<sup>-</sup> consumes an A<sup>0</sup> exciton, this simultaneously leads to a decrease in the A<sup>0</sup> exciton during the luminescence process. Moreover, it is well acknowledged that A<sup>-</sup> has a significantly lower luminescence probability than A<sup>0</sup>[28]. Consequently, the total PL intensity also decreases along with the attachment of the PCDA assembly and their in situ polymerization.

## 4 Conclusions

In summary, we have explored the modulation effect of organic self-assembled films on the properties of a hybridized semiconductor system. The investigated PCDA molecules play an electron donative role to the MoS<sub>2</sub>/TiO<sub>2</sub> compositional surface. Moreover, their assembly films can be further polymerized under proper excitations such as UV irradiation in this work. The polymerized PDA film possesses a highly conjugated skeleton and thus serves as a better electron donor to the surface. Their charge transfer to MoS<sub>2</sub> hence significantly varies the luminescence property of the latter. In this regard, we once again witness the effective and volatile modification effect of the organic films. Our results also emphasize that during the real designs as well as the practical applications of the functional hybridized systems, the interfacial interactions must be carefully considered.

## Acknowledgements

This work was supported by the National Natural Science Foundation of China (22172152, 21872130) and the National Key Research and Development Program of China (2021YFA1502801).

## Conflict of interest

The authors declare that they have no conflict of interest.

## Biographies

**Hechenyu Zha** received her master's degree from the School of Chemistry and Materials Science, University of Science and Technology of China, under the supervision of Prof. Xiang Shao. Her research mainly focused on the surface modification of metal oxide surface and its combination with two-dimensional materials.

**Xiang Shao** received his Ph.D. degree in Physical Chemistry from Peking University. He is currently a Professor at the University of Science and Technology of China. His research interests cover the surface chemistry of metal alloys, metal oxides and their combinations with two-dimensional materials.

## References

- [1] Li Y, Duerloo K A, Wauson K, et al. Structural semiconductor-to-semimetal phase transition in two-dimensional materials induced by electrostatic gating. *Nat. Commun.*, **2016**, 7: 10671.
- [2] Liu E, Fu Y, Wang Y, et al. Integrated digital inverters based on two-

- dimensional anisotropic ReS<sub>2</sub> field-effect transistors. *Nat. Commun.*, **2015**, 6: 6991.
- [3] Iqbal M W, Iqbal M Z, Khan M F, et al. Tailoring the electrical and photo-electrical properties of a WS<sub>2</sub> field effect transistor by selective n-type chemical doping. *RSC Adv.*, **2016**, 6 (29): 24675–24682.
- [4] Chen B, Meng Y H, Sha J W, et al. Preparation of MoS<sub>2</sub>/TiO<sub>2</sub> based nanocomposites for photocatalysis and rechargeable batteries: progress, challenges, and perspective. *Nanoscale*, **2018**, 10 (1): 34–68.
- [5] Li Y H, Cai C Z, Gu Y H, et al. Novel electronic properties of a new MoS<sub>2</sub>/TiO<sub>2</sub> heterostructure and potential applications in solar cells and photocatalysis. *Appl. Surf. Sci.*, **2017**, 414: 34–40.
- [6] Tu W G, Li Y C, Kuai L B, et al. Construction of unique two-dimensional MoS<sub>2</sub>-TiO<sub>2</sub> hybrid nanojunctions: MoS<sub>2</sub> as a promising cost-effective cocatalyst toward improved photocatalytic reduction of CO<sub>2</sub> to methanol. *Nanoscale*, **2017**, 9 (26): 9065–9070.
- [7] Xiang M M, Huang C X, Xing Y, et al. Modulated photoluminescence of single-layer MoS<sub>2</sub> on various rutile TiO<sub>2</sub> surfaces: implications for photocatalytic applications. *ACS Appl. Nano Mater.*, **2022**, 5 (5): 7609–7618.
- [8] Liu H H, Li Y, Xiang M M, et al. Single layered MoS<sub>2</sub> directly grown on rutile TiO<sub>2</sub>(110) for enhanced interfacial charge transfer. *ACS Nano*, **2019**, 13 (5): 6083–6089.
- [9] Kagan C R, Mitzi D B, Dimitrakopoulos C D. Organic-inorganic hybrid materials as semiconducting channels in thin-film field-effect transistors. *Science*, **1999**, 286 (5441): 945–947.
- [10] Jariwala D, Howell S L, Chen K S, et al. Hybrid, gate-tunable, van der Waals p-n heterojunctions from pentacene and MoS<sub>2</sub>. *Nano Lett.*, **2016**, 16 (1): 497–503.
- [11] Yu S H, Lee Y, Jang S K, et al. Dye-sensitized MoS<sub>2</sub> photodetector with enhanced spectral photoresponse. *ACS Nano*, **2014**, 8 (8): 8285–8291.
- [12] Yuan Y J, Lu H W, Ji Z G, et al. Enhanced visible-light-induced hydrogen evolution from water in a noble-metal-free system catalyzed by ZnTCPP-MoS<sub>2</sub>/TiO<sub>2</sub> assembly. *Chem. Eng. J.*, **2015**, 275: 8–16.
- [13] Guo C, Xue J D, Cheng L X, et al. Two-dimensional self-assembly of diacetylenic acid derivatives and their light-induced polymerization on HOPG surfaces. *Phys. Chem. Chem. Phys.*, **2017**, 19 (24): 16213–16218.
- [14] Giridharagopal R, Kelly K F. Substrate-dependent properties of polydiacetylene nanowires on graphite and MoS<sub>2</sub>. *ACS Nano*, **2008**, 2 (8): 1571–1580.
- [15] Okawa Y, Akai-Kasaya M, Kuwahara Y, et al. Controlled chain polymerisation and chemical soldering for single-molecule electronics. *Nanoscale*, **2012**, 4 (10): 3013–3028.
- [16] Liu H H. Direct fabrication of 2D materials on oxide surface and investigation of the interface properties. Thesis. Hefei: University of Science and Technology of China, **2018**. (in Chinese)
- [17] Yamamoto Y, Nakajima K, Ohsawa T, et al. Preparation of atomically smooth TiO<sub>2</sub> single crystal surfaces and their photochemical property. *Jpn. J. Appl. Phys.*, **2005**, 44 (17): L511–L514.
- [18] Wu J X, Liu J P, Cui J, et al. Dual-phase MoS<sub>2</sub> as a high-performance sodium-ion battery anode. *J. Mater. Chem. A*, **2020**, 8 (4): 2114–2122.
- [19] Lee C, Yan H, Brus L E, et al. Anomalous lattice vibrations of single- and few-layer MoS<sub>2</sub>. *ACS Nano*, **2010**, 4 (5): 2695–2700.
- [20] Ho Y T, Ma C H, Luong T T, et al. Layered MoS<sub>2</sub> grown on c-sapphire by pulsed laser deposition. *Phys. Status Solidi RRL*, **2015**, 9 (3): 187–191.
- [21] Ahn C, Lee J, Kim H U, et al. Low-temperature synthesis of large-scale molybdenum disulfide thin films directly on a plastic substrate using plasma-enhanced chemical vapor deposition. *Adv. Mater.*, **2015**, 27 (35): 5223–5229.

- [22] Hao S, Yang B C, Gao Y L. Unravelling merging behaviors and electrostatic properties of CVD-grown monolayer MoS<sub>2</sub> domains. *J. Chem. Phys.*, **2016**, *145* (8): 084704.
- [23] Mandal S K, Okawa Y, Hasegawa T, et al. Rate-determining factors in the chain polymerization of molecules initiated by local single-molecule excitation. *ACS Nano*, **2011**, *5* (4): 2779–2786.
- [24] Verveniatis E, Okawa Y, Makarova M V, et al. Self-assembling diacetylene molecules on atomically flat insulators. *Phys. Chem. Chem. Phys.*, **2016**, *18*: 31600–31605.
- [25] Splendiani A, Sun L, Zhang Y, et al. Emerging photoluminescence in monolayer MoS<sub>2</sub>. *Nano Lett.*, **2010**, *10* (4): 1271–1275.
- [26] Yuan Y J, Lu H W, Yu Z T, et al. Noble-metal-free molybdenum disulfide cocatalyst for photocatalytic hydrogen production. *ChemSusChem*, **2015**, *8* (24): 4113–4127.
- [27] van der Zande A M, Huang P Y, Chenet D A, et al. Grains and grain boundaries in highly crystalline monolayer molybdenum disulphide. *Nat. Mater.*, **2013**, *12* (6): 554–561.
- [28] Mak K F, He K, Lee C, et al. Tightly bound trions in monolayer MoS<sub>2</sub>. *Nat. Mater.*, **2013**, *12* (3): 207–211.